Carbohydrate Polymers 107 (2014) 167–173

Contents lists available at ScienceDirect

Carbohydrate Polymers

journal homepage: www.elsevier.com/locate/carbpol

Encapsulation of silver nanocomposites and effects of stabilizers

Ommer Bashir[a], Shokit Hussain[a], Zaheer Khan[a,*], Shaeel Ahmed AL-Thabaiti[b]

[a] Nanoscience Research Laboratory, Department of Chemistry, Jamia Millia Islamia (Central University), New Delhi 110025, India
[b] Department of Chemistry, Faculty of Science, King Abdul Aziz University, P.O. Box 80203, Jeddah 21589, Saudi Arabia

ARTICLE INFO

Article history:
Received 3 January 2014
Received in revised form 11 February 2014
Accepted 15 February 2014
Available online 23 February 2014

Keywords:
Silver nanocomposites
Encapsulation
Iodomerty
Starch

ABSTRACT

Silver nanocomposites (AgCPs) have been synthesized by chemical reduction from silver nitrate and sodium borohydride in presence of two stabilizers. Starch and poly (vinyl) alcohol, PVA with its rich source of polyhydroxy groups has been exploited for the capping of AgCPs. The ageing of $NaBH_4$ aqueous solution, molar ratios of the reactants, nature of the stabilizers, mixing order of $NaBH_4$ as well as capping agents have great influence on the morphology of AgCPs. We used the iodometric titration to conform the encapsulation of AgCPs inside the helical structure of starch. The reversible nature of encapsulation has been studied by UV–vis spectroscopic technique. Well-dispersed with an approximate size of 10 nm and aggregated with an approximate size of 24–52 nm AgCPs were observed in the absence and presence of stabilizers (starch and PVA), respectively. TEM images indicates that the reaction mixture containing different order of reactants and stabilizers ($PVA + NaBH_4 + Ag^+$, $PVA + Ag^+ + NaBH_4$, $starch + NaBH_4 + Ag^+$ and $starch + Ag^+ + NaBH_4$) have different morphology. Added electrolytes (NaCl, NaBr and NaI) do not detached the Ag^+ ions from the surface of AgNCs.

© 2014 Elsevier Ltd. All rights reserved.

1. Introduction

Synthesis of advanced metal nanoparticles in water or organic solvents using strong and weak reducing agents has been the interest of various researchers owing the wide range of applications (Henglein, 1989; Pileni, 1997; Grzelczak, Perez-Juste, Mulvaney & Liz-Marzan, 2008; Bakshi, 2011). Hyning and Zukoski studied the formation mechanism(s) of nanoscale silver nanoparticles produced by the reduction of silver perchlorate with ice-cold sodium borohydride solution and suggested that the reaction pathway does not follow classical nucleation and growth theory phenomenon (Van Hyning & Zukoski, 1998). Solomon described a laboratory method to the synthesis of yellow colloidal silver using ice-cold sodium borohydride (versatile strong reducing agent, $E^\circ = -1.33$ V versus NHE) for the reduction of Ag^+ ions into Ag° and to stabilize the monodisperse silver nanoparticles (Solomon, Bahadory, Jeyarajasingam, Rutkowsky & Boritz, 2007). Controlled synthesis of silver nanoparticles was not possible and/or difficult by the chemical reduction method of silver salts with strong reducing agents (Creighton, Blatchford, & Albrecht, 1979). Various chemical and seed-growth methods have been developed to obtain the desired and controlled morphology of silver and gold nanocomposites (Taton, Mirkin, & Letsinger, 2000; Nikoobakht & El-Sayed, 2001; Alkilany, Frey, Ferry, & Murphy, 2008; Bakshi, 2009; Ovando-Medinam et al., 2013). In the later technique a strong reducing agent, generally $NaBH_4$, is used to produce small metal particles, which are enlarged in a secondary step by further reduction with a weaker reducing agent(Chen, Wang, Ballato, Foulger, & Carroll, 2003). Shervani and Yamamoto reported a carbohydrate-directed synthesis of silver and gold nanocomposites, explained the effect of pH and different equivalent amounts of $NaBH_4$ on the morphology and color of gold nanocomposites (Shervani & Yamamoto, 2011). Mulvaney et al. prepared PVA films containing triangular and rod-shaped silver nanoparticles and used sodium borohydride, citrate, ascorbic acid and CTAB as the reducing agents and stabilizer, respectively (Wilson, Wilson, & Mulvaney, 2002). Among natural and synthetic polymers, the use of starch (fully biodegradable, consists 10–20% amylose forms a colloidal dispersion in hot water and amylopectin 80–90% completely water insoluble) (Shervani & Yamamoto, 2011; Vigneshwaran, Nachane, Balasubramanya, & Varadarajan, 2006; Shervani et al., 2008; Khan et al., 2013b) and PVA (biologically friendly water soluble polymer and has extremely low cytotoxicity) (Mbhele et al., 2003; Deng, Chen, Wang, & Ming, 2009) have been considered to the synthesis of silver and gold nanocomposites, which have potential applications in the fields of bioengineering, medical diagnosis and therapeutics like detection of genetic disorders (Cao, Jin, & Mirkin, 2002).

In the nanotechnology, stability of aqueous $NaBH_4$ solution is important for the transfer of hydrogen to the reductants, which leads to the formation of metal nanoparticles. In aqueous solution,

* Corresponding author. Tel.: +91 9911099077; fax: +91 11 26981717.
E-mail address: drkhanchem@yahoo.co.in (Z. Khan).

http://dx.doi.org/10.1016/j.carbpol.2014.02.055
0144-8617/© 2014 Elsevier Ltd. All rights reserved.

hydrolysis of $NaBH_4$ slows down with time because of the increasing concentration of the sodium hydroxide (Cloutier, Gyenge, & Alfantazi, 2007). Smirnova et al. determined the stability of alkaline aqueous solutions of sodium borohydride and reported that the degree of hydrolysis is 0.01% $NaBH_4$/h at room temperature in 1.0 N NaOH (Minkina, Shabunya, Kalinin, Martynenko, & Smirnova, 2012). Recently, we have used polymer, surfactants, starch and aqueous leaves extracts of various plants to stabilize the silver and gold nanoparticles using biomolecules (amino acids, organic acids, vitamin and glucose) and discussed the mechanism of quantum dots, trunicated triangular nanoplates, nanoflowers and nanowires formation (Khan & Talib, 2010; Rafey, Shrivastav, Iqbal, & Khan, 2011; Khan, Al-Thabaiti, Obaid, Khan, & Al-Youbi, 2011; Khan, Hussain, & Hashmi, 2012; Khan, AL-Thabaiti, El-Mossalamy, Hussain, & Obaid, 2013a). Our goal in this study was to investigate the effects of ageing $NaBH_4$ solution, starch, PVA and electrolytes on the morphology of AgNCs synthesized from $AgNO_3$ and $NaBH_4$ at room temperature. To the best of our knowledge, use of starch and PVA as a stabilizing and/or capping agent was reported for the first time on the Ag^+ –$NaBH_4$ redox reaction.

2. Experimental

2.1. Materials

Silver nitrate ($AgNO_3$, precursor to prepare silver nanoparticles, Merck India, 99.5%), sodium borohydride ($NaBH_4$, reductant, Merck India, 98%), starch, poly (vinyl) alcohol (stabilizers, Merck India) and inorganic electrolytes (NaCl, NaBr and NaI) were used as received without further purification. $AgNO_3$ solution was prepared by dissolving the required amount of $AgNO_3$ in 250 cm^3 distilled water and stored in an amber glass bottle. $NaBH_4$ solution (0.01 mol dm^3) was prepared by dissolving the required amounts in 50 cm^3 distilled water and used within the 1 h of the preparation time (*vide infra*). Stock PVA solutions were prepared by slow stepwise addition of PVA to deionized water whilst rapidly stirring to avoid the aggregation of PVA. Starch solution (2.0%) was prepared by dissolving the required amounts in the deionized water, boiled for 10 min in a 500 cm^3 Erlenmeyer flask with constant rapid stirring to avoid the aggregation of starch. The mixture was cooled and filtered with Whatman paper no. 1. Filtrate was collected and used.

2.2. Preparation and characterization of silver nanocomposites

Silver ions do not have any color, therefore, the formation of silver nanoparticles has been observed by a change in color since small nanoparticles of silver are yellow. In a typical experiment, silver nanoparticles were produced by dropping the $NaBH_4$ solution into $AgNO_3$ solution slowly. After all solutions were added, the spectra of mixed solutions were recorded at different time intervals by using UV–vis Recording Spectrophotometer, UV-260 Shimadzu, with 1 cm quartz cuvettes. An Accumet, Fisher Scientific digital pH meter 910 fitted with a combination electrode was used for pH measurements. Transmission electron microscope (JEOL, JEM-1011; Japan) was used for to determine the morphology of resulting AgNCs. For TEM measurements, samples were prepared by placing a drop of working solution on a carbon-coated standard copper grid (300 meshes) operating at 80 kV.

2.3. Encapsulation studies

Iodometric titration was used to find out the possible role of soluble starch during the synthesis of AgNCs. In a separate experiment, AgNCs were prepared by adding $AgNO_3$ (5.0 cm^3; 0.01 mol dm^{-3}) in a solution of $NaBH_4$ (1.0 cm^3; 0.01 mol dm^{-3}) and starch (1.0 cm^3; 2%). The resulting golden-yellow color (10 cm^3) was titrated against 0.1 N iodine solution (I_2/KI). The stable blue colour of starch-iodine complex was obtained, 2.0 cm^3 of AgNCs solution was further added in the blue color and the visible spectra were recorded at regular intervals.

3. Results and discussion

3.1. General considerations and stability of aqueous $NaBH_4$ solution

It is well known that molar ratio of Ag^+ ions to $NaBH_4$, ageing $NaBH_4$ solution, time of addition and order of mixing play an important role in the synthesis of silver and gold nanoparticles (Alkilany et al., 2008). Solomom used every day prepared $NaBH_4$ solution. Cloutier and Alfantazi reported that the water solutions of $NaBH_4$ contain certain amount of sodium hydroxide as a result of the $NaBH_4$ hydrolysis followed by the hydrolysis of sodium metaborate and $NaBH_4$ hydrolysis rate slows down with time because of the increasing concentration of the sodium hydroxide (Cao et al., 2002; Cloutier et al., 2007).

$$NaBH_4 + 2H_2O \longrightarrow NaBO_2 + 4H_2 \quad (1)$$

$$NaBO_2 + H_2O \longrightarrow NaOH + H_3BO_3 \quad (2)$$

Therefore, ageing time of $NaBH_4$ solutions is a crucial problem that we address first. In order to determine the exact ratio of Ag^+ to $NaBH_4$ and to establish a relation between the preparation time of $NaBH_4$ solutions and formation of silver nanoparticles, a series of experiments were carried out under different conditions (Table 1).

Table 1 indicated that different ratios of Ag^+ and $NaBH_4$ are responsible to the formation of prefect transparent, stable and different colored (gray, yellow-green and dark-brown) silver sols. Surprisingly, the breakdown of the silver sols took place in less than 1 h as the $[NaBH_4]/[Ag^+]$ decreases. On the other hand, stable and yellow colour silver sols (λ_{max} = 400 nm) were formed as the $[NaBH_4]/[Ag^+]$ increases at constant $[NaBH_4] = 10.0 \times 10^{-4}$ mol dm^{-3} (Table 1). Interestingly,

Table 1
Effects of molar ratios of reactants, ageing of $NaBH_4$ solutions and stabilizers on the visual formation of silver nanoparticles.

$[NaBH_4/Ag^+]$[a]	[Stabilizer]	Appearance and stability
0.2	0.0	Yellow to gray; 2 min; break down in 1 h
0.4	0.0	Gray; 2 min; break down in 1 h
0.6	0.0	Gray; color less after 2 h
0.8	0.0	Gray; color less after 2 h
1.0	0.0	Dark gray; color less after 1 h
2.5[b]	0.0	Yellowish-green stable
1.25[b]	0.0	Gray-greenish stable
1.66[b]	0.0	Light-gray stable
2.0[b]	0.0	Dark gray stable
5.0[b]	0.0	Yellow stable
0.2	0.2% starch 1 cm^3	Bright-yellow stable
0.4		Brown golden-yellow stable
0.6		Golden-brown stable
0.8		Dark golden-brown stable
1.0		Dark-brown stable even after over night
0.2	0.2% starch 10 cm^3	Bright-yellow stable
0.4		Brown golden-yellow stable
0.6		Golden-brown stable
0.8		Dark golden-brown stable
1.0		Dark-brown stable even after over night
0.2	0.2% starch 20 cm^3	Bright-yellow stable
0.2	0.2% PVA 1 cm^3	Golden-brown stable
0.2	0.2% PVA 10 cm^3	Golden-brown stable
0.2	0.2% PVA 20 cm^3	Golden-brown stable

[a] $[Ag^+]$ is constant (10.0×10^{-4} mol dm^{-3}) and $[NaBH_4]$ varying (from 2.0×10^{-4} to 10.0×10^{-4} mol dm^{-3}).
[b] $[NaBH_4]$ is constant (10.0×10^{-4} mol dm^{-3}) and $[Ag^+]$ varying (from 2.0×10^{-4} to 10.0×10^{-4} mol dm^{-3}).

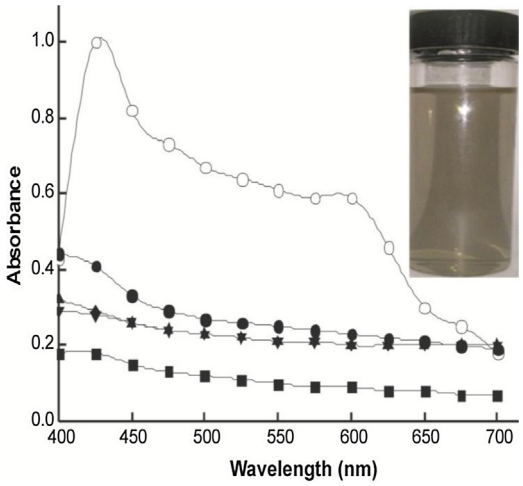

Fig. 1. Ageing effects of $NaBH_4$ solutions on the formation of silver nanoparticles as a function of preparation time. *Reaction conditions*: $[NaBH_4]/[Ag^+] = 0.2$, time = just after preparation (○), after 1 h (●), 2 h (•), 3 h (▲) and 15 h (■).

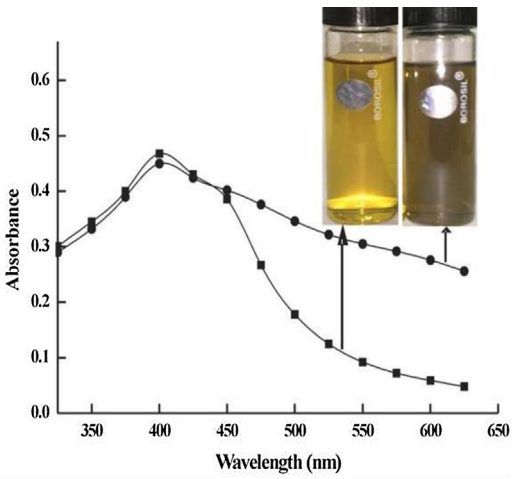

Fig. 2. Spectra of silver nanoparticles in presence of starch (■) and PVA (●). *Reaction conditions*: $[NaBH_4]/[Ag^+] = 0.2$, [starch or PVA] = 1.0 cm^3 of 2%.

it was observed that the color of reaction mixture containing $[Ag^+] = 10.0 \times 10^{-4}$ mol dm^{-3} and $[NaBH_4] = 2.0 \times 10^{-4}$ mol dm^{-3} changed very quickly (from colorless, pale yellow to greenish-gray) within the time of mixing, indicates the very fast reduction of Ag^+ ions into Ag°, which leads to the formation of colloidal silver. Fig. 1 shows the appearance of a single peak at 425 nm and a weak shoulder at 600 nm. The absorbance at 600 and 425 nm is an indicator of higher and lower wavelength absorbance which impart a darker solution color and a pale yellow color to the colloidal silver, respectively. As Fig. 1 show, at times higher than 1 h, the intensity of the 425 nm peak decreases. The intensity of surface plasmon resonance band decreases gradually with the ageing time of $NaBH_4$ solutions. We did not observe the appearances of any peak after 2 h for ageing $NaBH_4$ solutions (Fig. 1; ○, • and ■)

Under our experimental conditions, reverse order of reactant ($NaBH_4 + H_2O$ (for dilution) + $AgNO_3$ or $AgNO_3 + H_2O + NaBH_4$) addition does not alter the shape and position of the peak. Thus, the decrease in the absorbance and subsequent color transition might be due to the consumption of borohydride ions to produce a species that is not only more oxidizing (Van Hyning & Zukoski, 1998). Visual observations also suggested the evolution of hydrogen gas in the form of bubbles from the water solutions of $NaBH_4$. The pH of the freshly prepared $NaBH_4$ solution was found to be increased with ageing time (from 8.0, 8.3, 9.0 and 9.3 for time = just after preparation, 30 min, 1 h and 2 h, respectively and finally becomes constant after 24 h (pH 9.8), which is due to the increasing sodium hydroxide concentrations (Cao et al., 2002).

3.2. The effect of starch and PVA

To prepare the stable silver nanoparticles via the chemical reduction method, it is important to choose appropriate stabilizer and reducing agent. It is known that in the case of silver nanoparticles, the UV–vis absorption spectra are very sensitive to the particle size and their aggregation state, since the silver nanoparticles strongly absorb in the visible region due to surface plasmon resonance (Henglein, 1989; Bakshi, 2011; Solomon et al., 2007) Table 1 and visual observation showed that the typical color (from gray, bright yellow to yellowish-green) and stability of silver nanoparticles depends on the presence of stabilizer(s) as well as stochiometry of the reaction, which indicated the nanoparticle morphology altering with [stabilizers]. Therefore, effects of [starch and PVA] was studied at constant 1:5 ratio (Ag^+:$NaBH_4$) of the reactants. Fig. 2 shows the shape and position of the surface plasmon resonance band in presence of starch and PVA. Inspection of these data indicate that resulting gray color shows a band with band maximum at around 425 nm in absence of stabilizer (Fig. 1(●)). However, the spectrum of the silver nanoparticles shows the appearance of golden bright and yellowish-green colors with a sharp absorption peak at 400 nm (blue-shift of total 25 nm; Fig. 2) in presence of starch (■) and PVA (●), which is attributed to the characteristic spherical nanoparticles (Linnert, Mulvaney, Hanglein, & Weller, 1990). In addition to blue shift, the width of the band has also increased, which might be due to the excitation of different multiple modes present in faceted and anisotropic growth of particles. Fig. 2(■) also showed a weak hump at 450 along with a band. The presence of various absorption bands indicates the anisotropic growth of silver nanoparticles having various shapes, sizes with wide distribution (Zhang, Roll, Geddes, & Lakowicz, 2004). The digital images of the silver nanoparticles prepared in absence and presence of stabilizer(s) are shown in Figs. 1 and 2, respectively, indicating that the typical color of silver nanoparticles strongly depends on the nature and/or types of the stabilizers. The change in the position of wavelength maximal (boarding and blue-shifting) with [starch and/or PVA] (Fig. 2; Table 1) indicate that initially small or quantum dots of silver grow to form larger particles. Thus, we may safely conclude that the starch and PVA acted as a shape-directing agents and morphology depends on the small [stabilizer(s)]. The above results and explanations are in good agreement with the observations of Shervani and Yamamoto (Shervani & Yamamoto, 2011) and Patakfalvi et al. (Patakfalvi, Viranyi, & Dekany, 2004) to the shape-directing, stabilizing, and/or capping role of starch and PVA, respectively.

3.3. TEM images

Morphology of the silver nanoparticles that produced the spectra in Figs. 1 and 2 were determined by using TEM measurements. In order to establish the effect of mixing of stabilizers, TEM samples were taken at the same time from five separate experiments (order of mixing = (i) $NaBH_4 + Ag^+$, (ii) starch + $NaBH_4 + Ag^+$, (iii) starch + $Ag^+ + NaBH_4$, (iv) PVA + $NaBH_4 + Ag^+$, and (v) PVA + $Ag^+ + NaBH_4$). Fig. 3 shows typical TEM micrographs of the silver nanoparticles obtained by the Ag^+ ions (10.0×10^{-4} mol dm^{-3}) oxidation of $NaBH_4$ (10.0×10^{-4} mol dm^{-3}) with or without stabilizers. Nearly highly poly-dispersed dots with size from ≤6 nm and AgNPs from 12 nm to 145.46 nm were observed (Fig. 3A) in absence of stabilizers. The nanoplates (nanodisks) could be formed by the dissolution of the corner atoms of truncated triangular

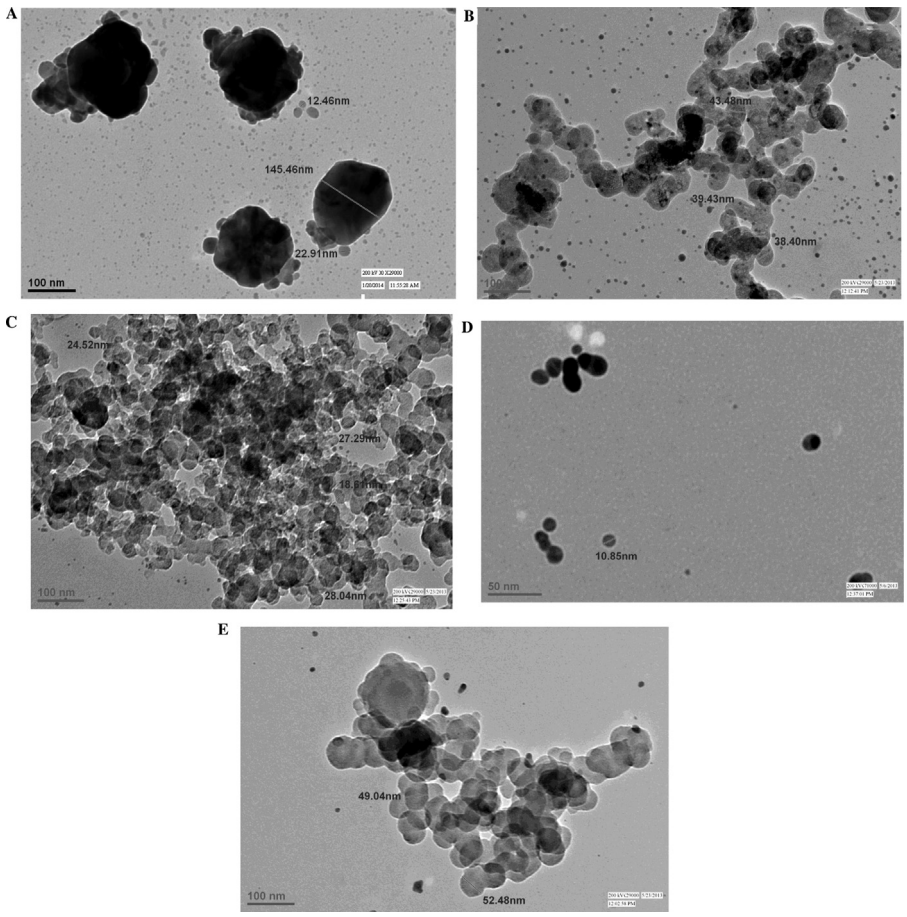

Fig. 3. Typical transmission electron micrograph of AgNCs in absence (A) and presence of stabilizers. *Reaction conditions:* $[NaBH_4]/[Ag^+] = 0.2$, [starch (B), (C) and PVA (D), (E)] = 1.0 cm^3 of 2%, order of mixing = starch + $NaBH_4$ + Ag^+ (B), starch + Ag^+ + $NaBH_4$ (C), PVA + $NaBH_4$ + Ag^+ (D), PVA + Ag^+ + $NaBH_4$ (E).

nanoplates (Fig. 3A). The polydispersity of the material might be due to the adsorption of borohydride (BH_4^-) anions onto the surface of silver nanoparticles. As a results, large number of BH_4^- adsorbed on the individual positive surface of silver nanoparticles through electrostatic interactions. Fig. 3A clearly suggest that BH_4^- ions acted both reducing as well as stabilizing agent and also responsible for the polydispersed nature of silver nanoparticles. The BH_4^- easily adsorbed to the silver particle to reduce electron density of surfaces and causes aggregation (Solomon et al., 2007).

Interestingly, two features are apparent from the TEMs in presence of stabilizer(s). First, the silver nanoparticles are spherical and poly-dispersed (Fig. 3B). Second, the spherical particles aggregated in an irregular manner, leads to the formation of beautiful silver. Such type of aggregation was not observed in Fig. 3A. All of the solution conditions, i.e., order of mixing of reactants and stabilizer(s) studied produced different TEMs showing different sizes, states of aggregation, and polydispersity (Fig. 3B–E for starch and PVA). A comparison between the TEMs images of starch with PVA shows that the particle size has drastically changed (from 18 nm to 38 nm and 10 nm to 52 nm, for starch and PVA, respectively) with order of mixing and the morphology has gone from roughly spherical to a highly irregular shape.

TEM image of Fig. 3B and C indicates the irregular aggregation of silver nanoparticles onto the surface of starch and also reveal that these silver nanoparticles aggregate beautifully in an unsymmetric manner to form the beautiful metallic silver. As can be seen from these TEM images (typical example), presence of irregular aggregated chains of silver nanoparticles provides the further evidence for the interparticle interaction (cross-linking) and/or aggregation. These results also conform that order of mixing (starch + Ag^+ + BH_4^-) leads to the formation of intense aggregated AgNCPs (Fig. 3C) might be due to the first ion-pair formation between lone-pairs of —OH groups of starch and Ag^+ ions and then reduction and aggregation of Ag^+ into Ag° occurred on the surface of helical structure of starch. The same behaviour was also observed for PVA + Ag^+ + BH_4^- system. The single-crystalloid nature of aggregated AgNPs were also confirmed by selected area electron diffraction patterns and indicated that the nanoplates were oriented with {1 1 1} planes as the basal plane (Fig. 4A and B). We did not observe the appearance of nanoplates and/or nanodisks in presence of starch and PVA.

In order to explain the mixing of the reactants and stabilizers on the morphology, presence of positive charge on Ag^+ ions and lone-pairs of electrons on —OH groups of stabilizer must be considered. It is certainly possible that the positive charge of Ag^+ forms an ion pair with the lone pairs of —OH groups present in the amylose and PVA polymer chain(s). Adsorption of AgNCs (Ag_4^{2+}) onto the amylase and/or PVA —OH groups through electrostatic interactions cannot be ruled out completely. Addition of amylase and/or PVA in a solution of Ag^+ ions inhibits the movement of free Ag^+ ions due to the coordination with —OH groups and providing favorable microenvironment for their capping, has been reported (Homan et al., 2011). Interestingly, Fig. 5 clearly shows a significant damping effect in the intensity of the plasmon peak in presence of PVA. These features are associated with the compact capping and tighten effect of PVA than that of amylose. It was well known that polymers, as protecting agents, are very effective to inhibit the agglomeration of particles (Khan, AL-Thabaiti, El- Mossalamy, & Obaid, 2009).

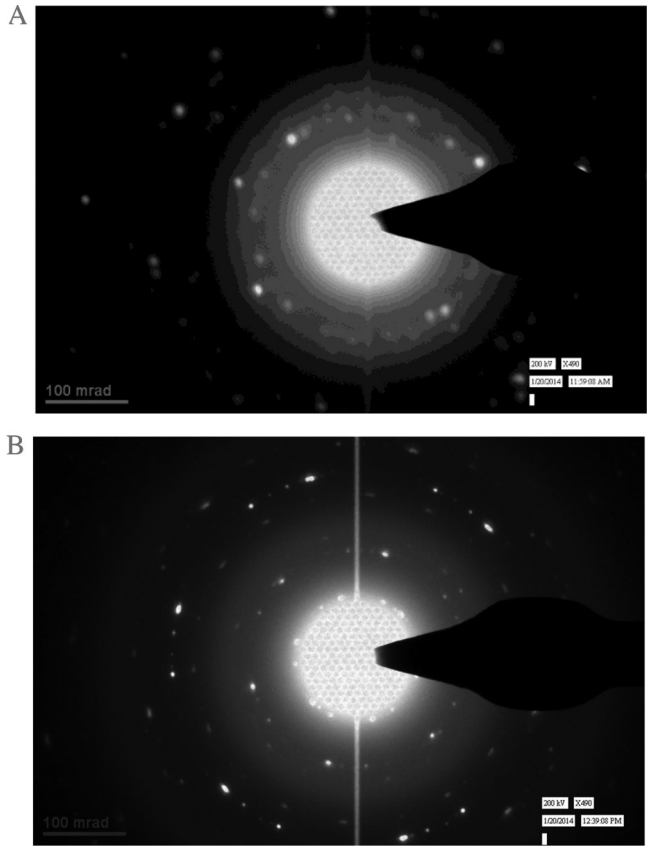

Fig. 4. Selected area electron diffraction pattern of AgNCs in absence (A) and presence of starch (B). *Reaction conditions:* $[NaBH_4]/[Ag^+] = 0.2$, [starch = 1.0 cm^3 of 2%, order of mixing = Ag^+ + starch + $NaBH_4$.

3.4. Stability of AgNCs

Table 1 show that the ratio to the reactants ($Ag^+/NaBH_4$) and presence of stabilizer(s) have great influence on the color and stability of AgNCs. In order to see more insight into the rate of the AgNCs formation, a series of kinetic experiments were performed to determine the time required for the reduction of Ag^+ ions by $NaBH_4$. The colourless reaction solution changes from pale yellow, gray to greenish-yellow was observed upon addition of Ag^+ ions to

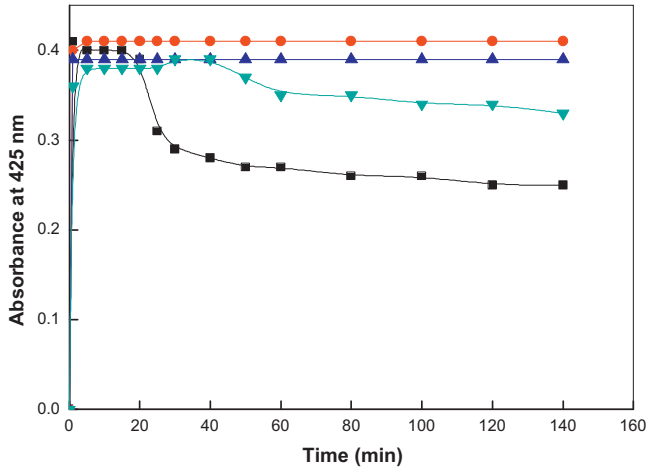

Fig. 5. Reaction-time plots to the formation of silver nanoparticles in absence (■ and •) and presence of stabilizers (▲ and ●). *Reaction conditions*: $[NaBH_4]/[Ag^+] = 0.2$ (■, ▲, and ●) and 5.0 (•), [starch (●) and PVA (▲)] = 1.0 cm^3 of 2%.

$$Ag^+ + BH_4^- + 3H_2O \xrightarrow{\text{fast}} Ag^0 + H_3BO_3 + 3.5\ H_2 \quad (3)$$

$$Ag^0 + Ag^+ \xrightarrow{\text{fast}} Ag_2^+ \quad (4)$$

$$2Ag_2^+ \xrightarrow{\text{fast}} Ag_4^{2+} \quad (5)$$

Ag_4^{2+} → BH_4^- → gray; starch → golden yellow; PVA → grayish yellow

Scheme 1. Effects of stabilizers on the growth of silver sols.

the $NaBH_4$ solution within the time of mixing at room temperature (25 °C). As can be seen in Fig. 5 (typical example), as the $[NaBH_4]$ (=10.0×10^{-4} mol dm^{-3}) was added, the absorbance of silver sol formation increases, becomes constant within 2 min, indicating that the both processes (nucleation and growth) have been completed within the time of mixing. The resulted AgNCs was stable for a long time in presence of stabiliser(s) (starch (●) and PVA (▲)). On the other hand, at 400 nm the absorbance increases very fast until it reaches a maximum, stable for some time and then decreased with reaction-time in absence of stabilizer (Fig. 5; (■ and•)). The decomposition rate constants were calculated from the slope of log (absorbance) versus time plot and found to be 2.5 and 1.2×10^{-5} s^{-1} for $[NaBH_4]/[Ag^+] = 0.2$ (■) and 5.0 (•), respectively. These results again confirmed that resulting AgNCs were unstable in absence of stabilizers and $[NaBH_4]$ has strong impact on the stability of AgNCs (Table 1) (Van Hyning & Zukoski, 1998; Solomon et al., 2007).

3.5. Mechanism

Mechanism to the reduction of silver nitrate by sodium borohydride in the presence of stabilizer(s), resulting in silver nanoparticles, followed the following Scheme 1.

Formation of various species of colloidal silver, Ag_2^+, Ag_3^{2+}, Ag_4^{2+}, Ag_8Ag^+ or Ag_9^+ and Ag_6^{4+}, in aqueous solution has been reported by Henglein and his co-workers. Out of these, Ag_4^{2+} is stable for a long time in presence of a polyanion even under air and growth stops at the stage of this species (Henglein, 1993). Therefore, Ag^+ form complex with Ag° (Eq. 4). Ag_2^+ species dimerize to give Ag_4^{2+} (Eq. 5). As a result, prefect transparent different colored AgNCs was formed in presence of different stabilizers.

3.6. Encapsulation studies

To ascertain the presence of Ag^+ ions (ionic silver in solution), aqueous solutions of NaCl, NaBr and NaI (5.0 cm^3; 0.01 mol dm^{-3}) were added to the solutions containing $NaBH_4$ 1.0 cm^3; 0.01 mol dm^{-3} + $AgNO_3$ 5.0 cm^3; 0.01 mol $dm^{-3}$with or without starch (2%, 1.0 cm^3) after 5 min following the mixing of silver to the sodium borohydride solution. Interestingly, not any precipitates (white, light yellow and dark yellow or any turbidity of AgCl, AgBr and AgI, respectively) was detected in presence of these electrolytes (solutions were non-opalescent before as well after the addition of Br^-, Cl^- and I^- as viewed by the naked eye; presence of ionic silver is the introduction of theses anions which will produce highly insoluble Ag–salts in the presence of Ag^+). On the other hand, we observed the appearance of white and yellowish turbidity after the addition of NaCl, NaBr and NaI in an aqueous $AgNO_3$ (5.0 cm^3; 0.01 mol dm^{-3}) solution. Fig. 6 also shows that the λ_{max} of the band remains unaffected in presence of added electrolytes but the intensity of band slightly decreased. These observations indicated

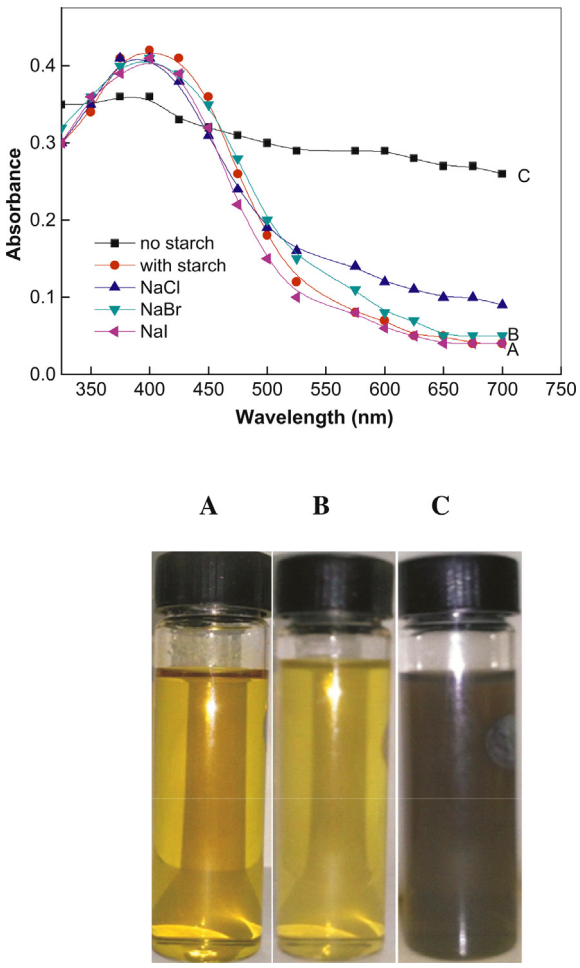

Fig. 6. Spectra and optical images of AgNCs in absence (■) and presence of starch (●) and effect of [electrolytes] = 0.04 mol dm^{-3} on the position surface Plasmon resonance band. *Reaction conditions*: $[NaBH_4]/[Ag^+] = 0.2$, [starch] = 1.0 cm^3 of 2%.

that essentially all Ag^+ ions were transformed to the Ag° and/or adsorbed on the surface of AgNCs within a short reaction-time and added Br^-, Cl^- and I^- ions could not detach the adsorbed Ag^+ from the surface of the resulting silver nanoparticles. The damping in the absorbance as a function of added adsorbate might be due to the chemisorptions onto the positive surface of AgNCs. The decrease in intensity on addition of various nucleophiles on the plasmon band has already been explained by Henglein (Henglein, 1993) as being due to a decrease in the mean-free path of electrons in silver colloids, donates the electron density to the particles via lone pairs of electrons, leading to a decrease in conductivity.

The results of iodometric titrations of starch-capped AgNCs were summarized in Fig. 7 as absorbance-wavelength profiles. The absorption spectrum of prepared AgNCs consists a single sharp band in the visible region at 400 nm (Fig. 7; (◯)), while the KI–I_2 regent covers the whole visible region of the spectrum and is light brown in color (Fig. 7; (▲)).Upon addition of 1 drop of 1.0 N KI–I_2 (iodine is not very soluble in water, therefore the iodine reagent is made by dissolving iodine in water in the presence of KI. This makes a linear triiodide ion complex which is soluble that slips into the coil of the starch causing an intense blue-black color) solution to a solution of golden-yellow colored of AgNCs (10.0 cm^3), the solution becomes pale yellow, the peak at 400 nm disappears completely and a new shoulder begins to develop in the vicinity 425 nm (Fig. 7; (■)) which might be due to the formation of poly-dispersed silver nanoparticles. Further, addition of one drop of the reagent, the same solution becomes deep-blue having two peaks at ca. 400 nm

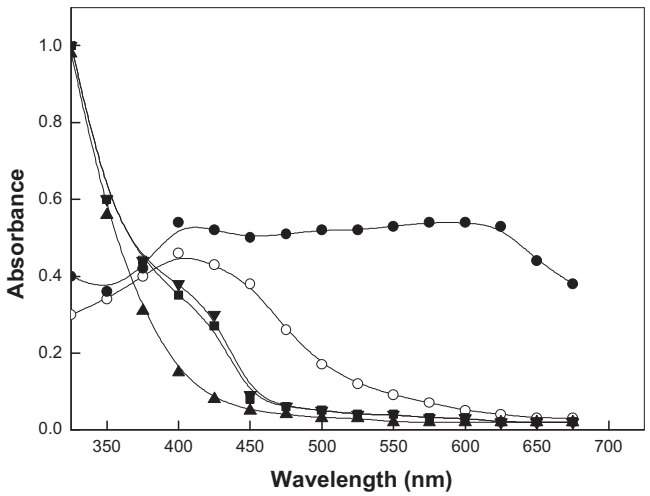

Fig. 7. Spectra of starch capped silver nanoparticles (◯) and KI–iodine (▲). The starch nanoparticles solution was titrated with iodine, and the spectra at various stages are as follows: addition of one drop KI–iodine reagent (yellow turbidity; ■), two drop (formation of blue starch–iodine complex; (●)) and the addition of excess silver nanoparticles resulting in the formation of yellow turbidity (•).

and 600 nm (Fig. 7; (●)). This deep-blue colour was due to the complexation between starch and iodine (Mendham, Denney, Barnes, & Thomas, 2000). A blue-black color results if starch contains amylase. If starch amylose is not present, then the color will stay orange or yellow. Starch amylopectin does not give the color. Further addition of 5.0 cm^3 of AgNCs in the same solution, the reaction mixture turned again pale-yellow resulting in the formation of a shoulder at 425 nm (Fig. 7; (•)). It thus seems that the AgNCs is rather unstable in presence of KI–I_2 reagent and is rapidly converted into larger particles, which might be due to the reversible encapsulation of silver nanoparticles. This red-shift is attributed to the strong interactions between the adsorbed Ag^+ and I^- ions on the surface of Ag_4^{2+}, vide infra, the nucleoplilicity of the I^- ion is better than that of Br^- or Cl^- ions (Al-Lohedan, Bunton, & Moffatt, 1983). The peak of starch-iodine complex at 585 nm disappeared completely. Our observations are in good agreement to the reversible encapsulation and the dissolved polyaniline as well as the composite could be recovered by replacement with molecular iodine (Sarma & Chattopadhyay, 2004). On the basis of Figs. 6 and 7 data, we may safely concluded that reaction proceeds through the formation of AgNCs, iodide–starch complex and finally silver nanoparticles detach the iodine from iodine–starch because the greater affinity of iodine towards silver in comparison to amylose respectively, (Fig. 7; (◯), (■), (●), and (•)) and starch encapsulated the AgNCs into its helical from structure as iodine in starch. A possible encapsulation mechanism (although highly schematic) could be that as shown in Scheme 2, which clearly indicates that, the probable role of amylose during the synthesis of AgNCs.

4. Conclusions

In this study we reported the reduction of silver nitrate by sodium borohydride in absence and presence of two stabilizers, namely starch and PVA. Upon mixing, all of the ionic silver is reduced immediately to form a different colored silver sol. Under our experimental conditions, ageing of $NaBH_4$ solution, order of reactant addition, dropping silver nitrate solution into $NaBH_4$ solution and presence of stabilizer(s), are important to obtain stable silver nanocomposites. In presence of starch and PVA, the particles grow to a stable size near 20–52 nm and, during this growth process, resulting in golden and yellowish-green solutions. The addition of NaCl, NaBr and NaI in the resulting silver sol does

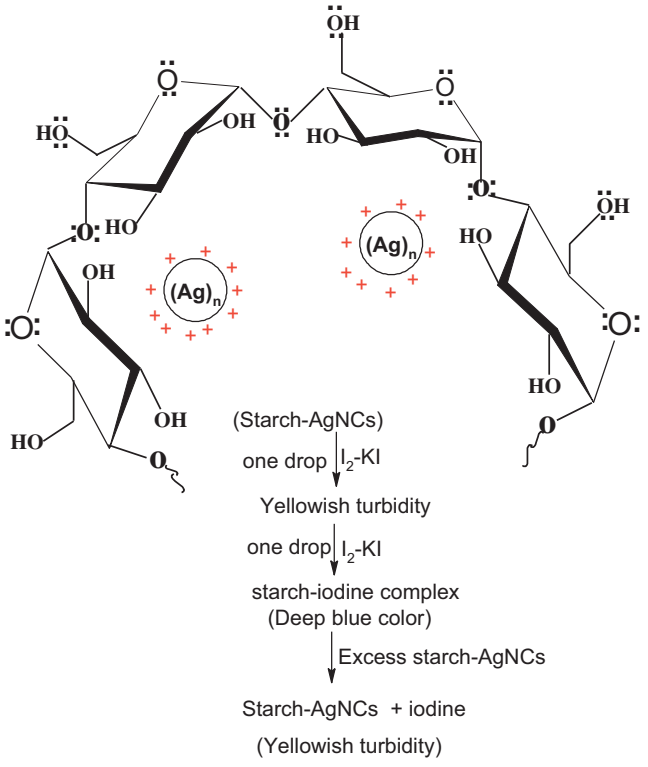

Scheme 2. Reversible encapsulation of AgNCs in starch.

not cause the immediate precipitation of silver halides. It is also reported that encapsulated silver nano-composites in starch could be recovered by replacement with molecular iodine. The binding interaction between soluble starch and silver nano-composites is relatively weak compared to the interaction between the Ag° and Ag^{+} ions. The use of different stabilizers offers numerous benefits to obtained different colored silver sols having widespread morphology.

References

Alkilany, A. M., Frey, R. L., Ferry, J. L., & Murphy, C. J. (2008). Gold nanorods as nanoadmicelles: 1-Naphthol partitioning into a nanorod-bound surfactant bilayer. *Langmuir*, *24*, 10235–10239.

Al-Lohedan, H., Bunton, C. A., & Moffatt, J. R. (1983). Quantitative treatment of micellar effects upon the nucleophilicity of halide ions. *Journal of Physical Chemistry*, *87*, 332–335.

Bakshi, M. S. (2009). A simple method of superlattice formation: Step-by-step evaluation of crystal growth of gold nanoparticles through seed-growth method. *Langmuir*, *25*, 12697–12705.

Bakshi, M. S. (2011). Nanoshape control tendency of phospholipids and proteins: Protein – Nanoparticle composites, seeding, self-aggregation, and their applications in bionanotechnology and nanotoxicology. *Journal of Physical Chemistry C*, *115*, 13947–13960.

Cao, Y. C., Jin, R., & Mirkin, C. A. (2002). Nanoparticles with Raman spectroscopic fingerprints for DNA and RNA detection. *Science*, *297*, 1536–1540.

Chen, S. H., Wang, Z. L., Ballato, J., Foulger, S. H., & Carroll, D. L. (2003). Monopod, bipod, tripod, and tetrapod gold nanocrystals. *Journal of American Chemical Society*, *125*, 16186–16187.

Cloutier, C. R., Gyenge, E., & Alfantazi, A. (2007). Physicochemical properties of alkaline aqueous sodium metaborate solutions. *Journal of Fuel Cell Science and Technology*, *4*, 88–98.

Creighton, J. A., Blatchford, C. G., & Albrecht, M. G. (1979). Plasma resonance enhancement of Raman scattering by pyridine adsorbed on silver or gold sol particles of size comparable to the excitation wavelength. *Journal of the Chemical Society, Faraday Transactions 2: Molecular and Chemical Physics*, *75*, 790–798.

Deng, Y., Chen, C., Wang, P., & Ming, H. (2009). Field enhancement and large optical nonlinearity in Ag nanocomposite polymer film. *Journal of Modern Optics*, *56*, 1000–1003.

Grzelczak, M., Perez-Juste, J., Mulvaney, P., & Liz-Marzan, L. M. (2008). Shape control in gold nanoparticle synthesis. *Chemical Society Reviews*, *37*, 1783–1791.

Henglein, A. (1993). Physicochemical properties of small metal particles in solution: "Microelectrode" reactions, chemisorption, composite metal particles, and the atom-to-metal transition. *Journal of Physical Chemistry*, *97*, 5457–5471.

Henglein, A. (1989). Small-particle research: Physicochemical properties of extremely small colloidal metal and semiconductor particles. *Chemical Reviews*, *89*, 1861–1873.

Khan, Z., AL-Thabaiti, S. A., El-Mossalamy, E. H., Hussain, J. I., & Obaid, A. Y. (2013). Effects of electrolytes and surfactants on the morphology and stability of advanced silver nano-materials. *Materials Research Bulletin*, *48*, 1137–1142.

Khan, Z., AL-Thabaiti, S. A., El-Mossalamy, E. H., & Obaid, A. Y. (2009). Effect of macromolecule poly (vinyl alcohol) on the growth of cetyltrimethylammonium bromide stabilized Ag-nanoparticles. *Colloids and Surfaces A: Physicochemical and Engineering Aspects*, *352*, 31–37.

Khan, Z., Al-Thabaiti, S. A., Obaid, A. Y., Khan, Z. A., & Al-Youbi, A. O. (2011). Effects of solvents on the stability and morphology of CTAB-stabilized silver nanoparticles. *Colloids and Surfaces A: Physicochemical and Engineering Aspects*, *390*, 120–125.

Khan, Z., Hussain, J. I., & Hashmi, A. A. (2012). Shape-directing role of cetyltrimethylammonium bromide in the green synthesis of Ag-nanoparticles using neem (*Azadirachta indica*) leaf extract. *Colloids and Surfaces B: Biointerfaces*, *95*, 229–234.

Khan, Z., Singh, T., Hussain, J. I., Obaid, A. Y., Al-Thabaiti, S. A., & El-Mossalamy, E. H. (2013). Starch-directed green synthesis, characterization and morphology of silver nanoparticles. *Colloids and Surfaces B: Biointerfaces*, *102*, 578–584.

Khan, Z., & Talib, A. (2010). Growth of different morphologies (quantum dots to nanorod) of Ag-nanoparticles: Role of cysteine concentrations. *Colloids and Surfaces B: Biointerfaces*, *76*, 164–169.

Linnert, T., Mulvaney, P., Hanglein, A., & Weller, H. (1990). Long-lived nonmetallic silver clusters in aqueous solution: Preparation and photolysis. *Journal of the American Chemical Society*, *112*, 4657–4664.

Mbhele, Z. H., Salemane, M. G., van Sittert, C. G. C. E., Nedeljkovic, J. M., Djokovic, V., & Luyt, A. S. (2003). Fabrication and characterization of silver-polyvinyl alcohol nanocomposites. *Chemistry of Materials*, *15*, 5019–5024.

Mendham, J., Denney, R. C., Barnes, J. D., & Thomas, M. J. K. (2000). *Vogel's quantitative chemical analysis* (6th ed.). New York: Prentice Hall. ISBN 0-582-22628-7.

Minkina, V. G., Shabunya, S. I., Kalinin, V. I., Martynenko, V. V., & Smirnova, A. L. (2012). Stability of alkaline aqueous solutions of sodium borohydride. *International Journal of Hydrogen Energy*, *37*, 3313–3318.

Nikoobakht, B., & El-Sayed, M. A. (2001). Evidence for bilayer assembly of cationic surfactants on the surface of gold nanorods. *Langmuir*, *17*, 6368–6374.

Ovando-Medinam, V. M., Martinez-Gutierrez, H., Corona-Rivera, M. A., Cervantes-González, E., Flores-Mejia, J., & Farias-Cepeda, L. (2013). Silver/silver bromide/polypyrrole nanoparticles obtained by microemulsion photopolymerization in the presence of a cationic surfactant. *Colloid and Polymer Science*, *291*, 2131–2138.

Patakfalvi, R., Viranyi, Z., & Dekany, I. (2004). Kinetics of silver nanoparticle growth in aqueous polymer solutions. *Colloid and Polymer Science*, *283*, 299–305.

Pileni, M. P. (1997). Nanosized particles made in colloidal assemblies. *Langmuir*, *13*, 3266–3276.

Rafey, A., Shrivastav, K. B. L., Iqbal, S. A., & Khan, Z. (2011). Growth of Ag-nanoparticles using aspartic acid in aqueous solutions. *Journal of Colloid and Interface Science*, *354*, 190–195.

Sarma, T. K., & Chattopadhyay, A. (2004). Reversible encapsulation of nanometer-size polyaniline and polyaniline – Au-nanoparticle composite in starch. *Langmuir*, *20*, 4733–4737.

Shervani, Z., Ikushima, Y., Sato, M., Kawanami, H., Hakuta, Y., Yokoyama, T., et al. (2008). Morphology and size-controlled synthesis of silver nanoparticles in aqueous surfactant polymer solutions. *Colloid and Polymer Science*, *286*, 403–410.

Shervani, Z., & Yamamoto, Y. (2011). Carbohydrate-directed synthesis of silver and gold nanoparticles: Effect of the structure of carbohydrates and reducing agents on the size and morphology of the composites. *Carbohydrate Research*, *346*, 651–658.

Solomon, S. D., Bahadory, M., Jeyarajasingam, A. v., Rutkowsky, S. A., & Boritz, C. (2007). Synthesis and study of silver nanoparticles. *Journal of Chemical Education*, *84*, 322–325.

Taton, T. A., Mirkin, C. A., & Letsinger, R. L. (2000). Scanometric DNA array detection with nanoparticle probes. *Science*, *289*, 1757–1760.

Van Hyning, D. L., & Zukoski, C. F. (1998). Formation mechanisms and aggregation behavior of borohydride reduced silver particles. *Langmuir*, *14*, 7034–7046.

Vigneshwaran, N., Nachane, R. P., Balasubramanya, R. H., & Varadarajan, P. V. (2006). A novel one-pot 'green' synthesis of stable silver nanoparticles using soluble starch. *Carbohydrate Research*, *341*, 2012–2018.

Wilson, O., Wilson, G. J., & Mulvaney, P. (2002). Laser writing in polarized silver nanorod films. *Advanced Materials*, *14*, 1000–1004.

Zhang, J., Roll, D., Geddes, C. D., & Lakowicz, J. R. (2004). Aggregation of silver nanoparticle – Dextran adducts with concanavalin A and competitive complexation with glucose. *The Journal of the Physical Chemistry B*, *108*, 12210–12214.